Supporting Information

Comparative study of molecular beam epitaxy-deposited ZnS:O and CdS:O as electron-transporting materials in $Sb_2(S,Se)_3$ solar cells

Ke Li,[abc] *Zhihao Yan,*[d] *Yawu He,*[b] *Haolin Wang,*[b] *Dan Liu,*[b] *Jiabin Dong,*[e] *Yi Zhang,*[e] *Rongfeng Tang,*[b] *Xiuxun Han,**[ac] *and Tao Chen**[b]

[a] Institute of Optoelectronic Materials and Devices, School of Materials Science and Engineering, Jiangxi University of Science and Technology, Ganzhou 341000, P. R. China.

[b] Hefei National Research Center for Physical Sciences at the Microscale, CAS Key Laboratory of Materials for Energy Conversion, Department of Materials Science and Engineering, School of Chemistry and Materials Science, University of Science and Technology of China, Hefei, Anhui 230026, P. R. China.

[c] National Rare Earth Function Materials Innovation Center, Ganzhou 341100, P. R. China.

[d] College of Materials Science and Opto-Electronic Technology, University of Chinese Academy of Sciences, Beijing 100049, P. R. China.

[e] Institute of Photoelectronic Thin Film Devices and Technology, State Key Laboratory of Photovoltaic Materials and Cells, and Engineering Research Center of Thin Film Optoelectronics Technology, Ministry of Education, Nankai University, Tianjin 300350, P. R. China.

*E-mail: tchenmse@ustc.edu.cn; xxhan@jxust.edu.cn

Note S1. Morphology and crystallinity analysis of ZnS films prepared by MBE (MBE-ZnS) and CBD methods (CBD-ZnS).

We characterized the morphology of CBD- and MBE-ZnS films by field emission scanning electron microscopy (SEM), as shown in Fig. S1a–d, both films consist of ZnS grains, and MBE-ZnS films have larger grain sizes compared to CBD-ZnS. The statistical results show that the grain size of CBD- and MBE-ZnS films are 19 ± 3 and 50 ± 12 nm, respectively (Fig. S1e), which implies the improvement of the crystallinity of MBE-ZnS films. The annealed CBD- and MBE-ZnS films were characterized by X-ray diffraction (XRD) to demonstrate the crystallinity of the films. To exclude the disturbance of the intense FTO diffraction peaks, we deposited the films onto quartz glass, and the results are shown in Fig. S1f. For the MBE-ZnS film, diffraction peaks are observed at 28.5°, 33.1°, 47.5°, and 56.3°, which are attributed to the (111), (200), (220), and (311) crystal planes of cubic ZnS phase (PDF#99-0097), respectively, however, no diffraction peaks are observed in the CBD-ZnS film. The above results demonstrate that MBE-ZnS films have much higher crystallinity than CBD-ZnS, which makes MBE-ZnS more promising for application in solar cells.

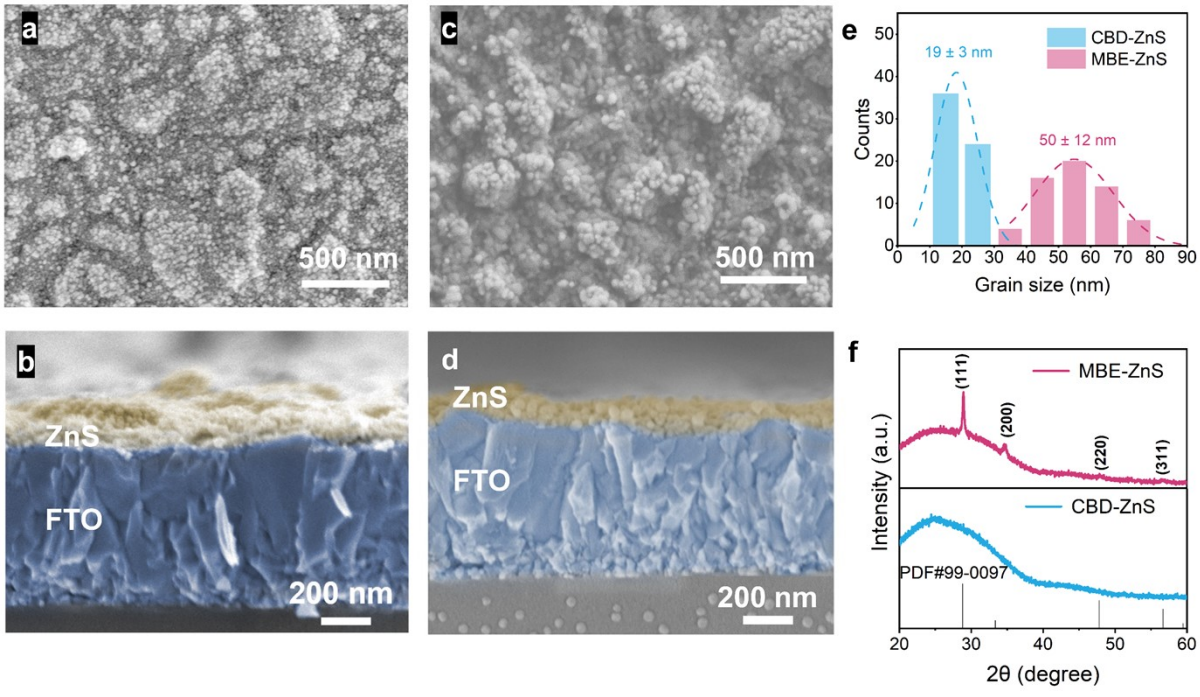

Fig. S1 Top view and cross-sectional SEM images of (a,b) CBD-ZnS and (c,d) MBE-ZnS films. (e) Grain size distribution of CBD- and MBE-ZnS films. (f) XRD patterns of annealed CBD- and MBE-ZnS films deposited on quartz glass substrate.

Note S2. Calculation details of texture coefficient.

The texture coefficient (TC) of the film is calculated by the following equation:[1]

$$TC(hkl) = \left(\frac{I_{(hkl)}/I_{r(hkl)}}{[(1/n)\sum I_{(hkl)}/I_{r(hkl)}]} \right) \#(S1)$$

where $I_{(hkl)}$, $I_{r(hkl)}$, and n indicate the X-ray diffraction intensities obtained from the film, the intensity of the reference diffraction pattern (inorganic crystal structure database 15236 and 22176), and the considered number of diffraction peaks, respectively.

Note S3 Calculation details of conduction band minimum, valence band maximum, and Fermi level.

The conduction band minimum (E_C), the valence band maximum (E_V), and the Fermi level (E_F) of the films are calculated according to the following equations:

$$\varphi = h\nu - E_{cutoff} \#(S2)$$

$$E_F = E_{vac} - \varphi \#(S3)$$

$$E_V = E_F - E_{onset} \#(S4)$$

$$E_C = E_V + E_g \#(S5)$$

where φ represents the work function of the ZnS films, $h\nu$ represents the photon energy of the synchrotron radiation BL 10B beamline (150 eV), E_{vac} represents the vacuum level (0 eV), and the and the E_g of the ZnS films is obtained from the fitting results in Fig. S2.

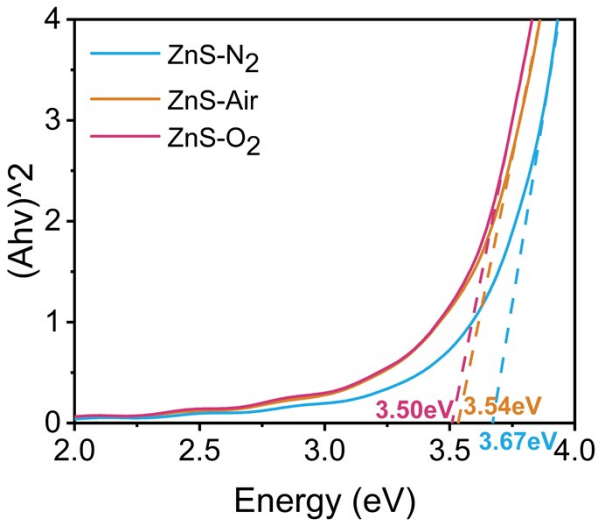

Fig. S2 Tauc plots of the UV-vis absorption spectra of the above ZnS films.

Table S1 E_C, E_V, and E_F of the ZnS-N_2, ZnS-Air, and ZnS-O_2 films.

	E_C/eV	E_V/eV	E_F/eV	E_g/eV
ZnS-N_2	-3.32	-6.99	-3.87	3.67
ZnS-Air	-3.46	-7.00	-4.20	3.54
ZnS-O_2	-3.62	-7.12	-3.81	3.50

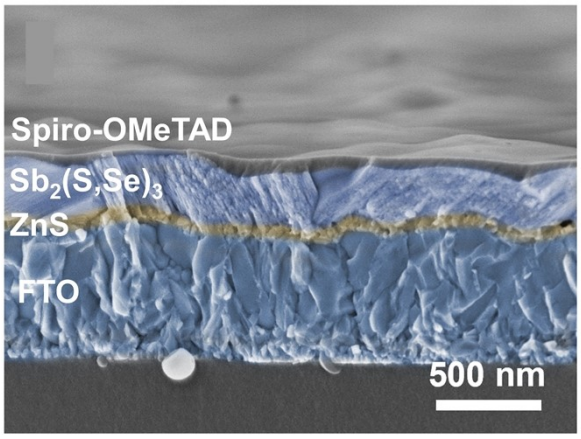

Fig. S3 Cross-section SEM image of the ZnS/$Sb_2(S,Se)_3$ superstrate solar cell devices.

Table S2 Photovoltaic parameters of $Sb_2(S,Se)_3$ solar cell devices based on ZnS-N_2, ZnS-Air, and ZnS-O_2 films.

Sample	V_{OC} (V)	J_{SC} (mA cm^{-2})	FF (%)	PCE (%)
	0.673	3.61	25.67	0.62
	0.682	3.94	26.84	0.72
	0.691	4.12	27.74	0.79
	0.692	2.27	24.78	0.39
ZnS-N_2	0.700	2.77	25.72	0.50
	0.673	4.74	27.98	0.89
	0.691	2.50	25.36	0.44
	0.682	4.31	27.87	0.82
	0.682	4.62	28.58	0.90

	0.595	14.71	33.47	2.93
	0.518	14.62	32.60	2.47
	0.578	14.37	28.17	2.34
	0.561	13.91	31.09	2.43
ZnS-Air	0.518	13.50	28.60	2.00
	0.578	12.46	30.87	2.22
	0.500	11.53	41.77	2.41
	0.573	10.62	41.84	2.55
	0.509	10.11	39.28	2.02
	0.589	19.80	43.37	5.05
	0.595	17.81	46.66	4.94
	0.563	18.76	48.80	5.15
	0.599	17.98	43.52	4.69
$ZnS-O_2$	0.589	18.98	43.24	4.83
	0.563	17.91	47.01	4.74
	0.555	18.04	49.07	4.91
	0.563	18.23	47.83	4.91
	0.597	18.24	43.55	4.75

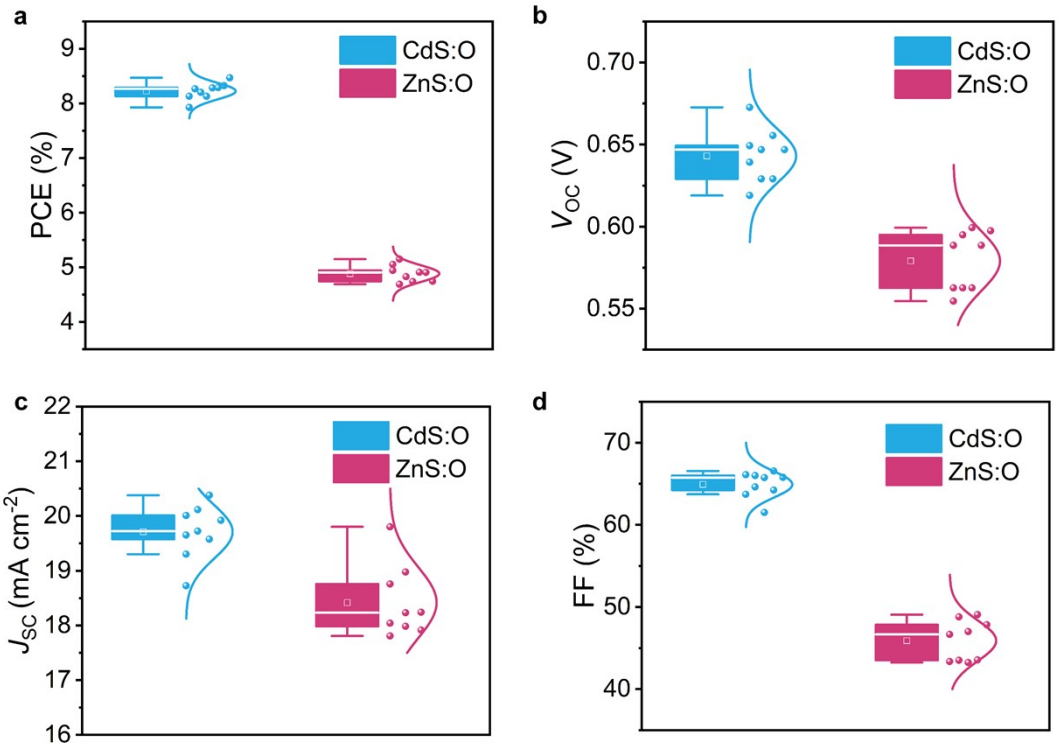

Fig. S4 Statistical boxplots of (a) PCE, (b) V_{OC}, (c) J_{SC}, and (d) FF for CdS:O- and ZnS:O-based $Sb_2(S,Se)_3$ solar cells.

Table S3 Photovoltaic parameters of $Sb_2(S,Se)_3$ solar cell devices based on CdS:O and ZnS:O films.

Sample	V_{OC} (V)	J_{SC} (mA cm^{-2})	FF (%)	PCE (%)
CdS:O	0.649	19.65	63.71	8.13
	0.639	20.01	64.63	8.27
	0.629	19.72	66.10	8.20
	0.629	19.57	66.00	8.13
	0.673	18.72	65.76	8.28
	0.619	20.12	66.56	8.29
	0.647	19.92	61.51	7.93
	0.655	19.30	65.79	8.32
	0.647	20.38	64.24	8.47
ZnS:O	0.589	19.80	43.37	5.05
	0.595	17.81	46.66	4.94

	0.563	18.76	48.80	5.15
	0.599	17.98	43.52	4.69
	0.589	18.98	43.24	4.83
	0.563	17.91	47.01	4.74
	0.555	18.04	49.07	4.91
	0.563	18.23	47.83	4.91
	0.597	18.24	43.55	4.75

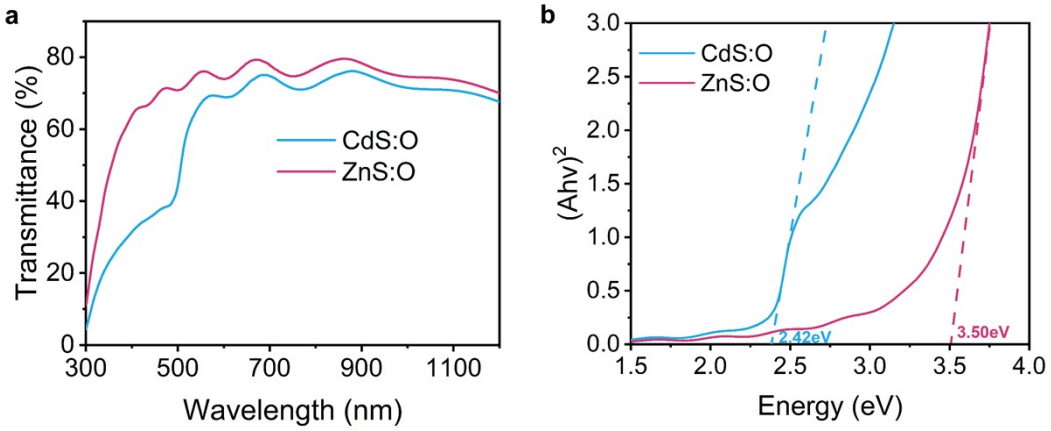

Fig. S5 (a) Transmittance spectra and (b) Tauc plots of UV-Vis absorption spectra of CdS:O and ZnS:O films.

Table S4 E_C, E_V, E_F,and E_g of CdS:O and ZnS:O films (E_g is obtained from Tauc plots of UV-vis absorption spectra in Fig. S5b).

Sample	E_C/eV	E_V/eV	E_F/eV	E_g/eV
CdS:O	-3.84	-6.24	-3.96	2.40
ZnS:O	-3.62	-7.12	-3.81	3.50

Table S5 Lattice mismatches between different crystal forms of CdS and ZnS with Sb_2S_3.

Sample	Lattice constant (Å)			Lattice mismatch
	a	b	c	
Sb_2S_3	11.239	11.313	3.8411	
C-CdS	5.832	5.832	5.832	41.2%
H-CdS	4.14092	4.14092	6.7198	7.5%
C-ZnS	5.4145	5.4145	5.4145	34.0%
H-ZnS	3.836	3.836	6.277	0.13%

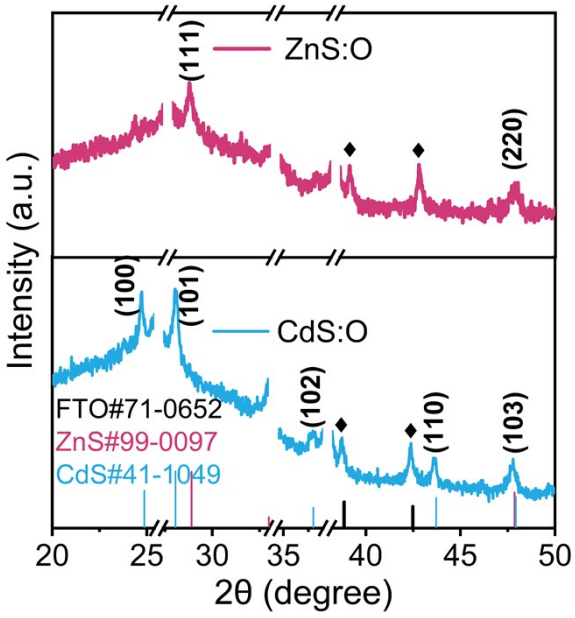

Fig. S6. XRD patterns of CdS:O and ZnS:O films deposited on FTO substrates by MBE method. The diffraction peaks of CdS:O are attributed to the hexagonal CdS phase (PDF#41-1049), and the diffraction peaks of ZnS:O are ascribed to the cubic ZnS phase (PDF#99-0097).

Note S4. TAS measurement details

The kinetic curves are normalized and fitted by a biexponential decay kinetic model with the following fitting equation:[2]

$$\Delta A(t) = \sum_{i=1}^{2} A_i \exp\left(-t/\tau_i\right) \#(S6)$$

where ΔA represents the change in absorption of the sample after applying the pump pulse, t is the detection delay time, A_i represents the amplitude, and τ_i represents the decay lifetime. The average carrier lifetime (τ_{ave}) is calculated by the following equation:

$$\tau_{ave} = \frac{\sum_{i=1}^{2} A_i \tau_i^2}{\sum_{i=1}^{2} A_i \tau_i} \#(S7)$$

References

1 D. Aryanto, P. Marwoto, T. Sudiro, A. S. Wismogroho, and Sugianto, *J. Phys. Conf. Ser.*, 2019, **1191**, 012031.

2 H. Cai, R. Cao, J. Gao, C. Qian, B. Che, R. Tang, C. Zhu and T. Chen, *Adv. Funct. Mater.*, 2022, **32**, 2208243.